Lasing Characteristics of GaInAsP–InP Strained Quantum-Well Microdisk Injection Lasers with Diameter of 2–10 μm

Toshihiko Baba, *Member, IEEE,* Masayuki Fujita, Atsushi Sakai, Mitsuhiro Kihara, and Ryoh Watanabe

***Abstract*— We have obtained the pulsed lasing operation in 2–5-μm diameter microdisk injection lasers using GaInAsP–InP compressive-strained multiple-quantum-well (MQW) wafer around room temperature. The effective cavity volume of the 2-μm-diameter device is the smallest among those for any types of electrically-pumped lasers. The threshold current of this device was as low as 0.2 mA. Cavity modes in emission spectra observed under cw condition coincides well with theoretically predicted whispering gallery modes. Further reduction of diameter to less than 1.5 μm will realize the condition for spontaneous emission almost coupling into a single mode, which results in the thresholdless lasing operation.**

***Index Terms*—GaInAsP–InP, microcavity, microdisk, semiconductor laser, whispering gallery mode.**

I. Introduction

SPONTANEOUS EMISSION control [1]–[4] is of great interest since it provides novel high performance in laser diodes, e.g., thresholdless operation and high-speed modulation without relaxation oscillation. It is realized in a microcavity whose effective volume V satisfies single-mode condition $V \leqq \lambda^4/(2\pi^2 n^3 \Delta\lambda)$, where λ is the resonant wavelength, n the effective refractive index of cavity, and $\Delta\lambda$ the spectral width given by the full-width at half-maximum (FWHM) of atomic radiation spectrum. Microdisk lasers [5]–[7] are promising candidates that realize this condition since their effective cavity thickness is easily reduced to nearly $\lambda/2n$ by the strong optical confinement into the thin disk layer. This simplifies the requirement for disk diameter; it is 1–2 μm for $\lambda = 1.55$ μm and $\Delta\lambda = 100$ nm. It is much larger than the diameter required for air-post vertical cavity surface emitting lasers, i.e., smaller than 0.4 μm [8].

So far, photo-pumped lasing in a 1.6-μm-diameter device has been reported and the spontaneous emission factor defined by the coupling efficiency of spontaneous emission energy into a single lasing mode has been discussed [7]. The fabrication of injection-type devices of 5–9 μm in diameter has also been reported [5]. However, the demonstration of lasing operation was limited to no smaller than 9 μm. In this study, we obtained the pulsed lasing operation for injection-type devices of 2–10 μm in diameter. The cavity volume of the smallest one is very close to the single-mode condition. We also observed resonant modes in emission spectra under continuous-wave (CW) condition, which coincide with theoretical ones obtained by a simple two-dimensional (2-D) model. From these results, we discuss the potential of this kind of device for the spontaneous emission control.

Manuscript received December 4, 1996; revised March 17, 1997.

The authors are with the Yokohama National University, Division of Electrical and Computer Engineering, Hodogayaku, Yokohama 240, Japan.

Publisher Item Identifier S 1041-1135(97)04916-1.

Fig. 1. SEM photograph of fabricated 2-μm-diameter device.

II. Fabrication Process and Lasing Characteristics

In this experiment, we prepared GaInAsP–InP compressive-strained multiple-quantum-well (CS-MQW) wafer grown on (001) n-InP substrate by metal organic chemical vapor deposition. Each thickness of quaternary (Q) well layers was 3–4 nm and that of 1.2-μm-Q barrier layers 10 nm. The strain was 1%, and the number of wells was four. The total thickness of active layer including 50-nm-thick 1.2-μm-Q guide layers and 30-nm-thick 1.1-μm-Q gradient index (GRIN) layers was nearly 0.2 μm. We expected the GRIN layers to help the smooth carrier injection into the wells and to suppress the carrier leakage at disk surfaces by the surface recombination. The peak emission wavelength was 1.545 μm. Between the substrate and n-InP cladding below the active layer, 0.3-μm-thick n-GaInAs was inserted in order to stop the wet chemical etching described below. On p-InP cladding above the active layer, 1-μm-thick p-GaInAs was grown as a contact layer.

On the substrate surface we evaporated AuGe, while on the epitaxial surface Au–Zn–Au–Ti. We patterned the Ti film into circular dot shapes by CF_4 reactive ion etching. Through this film, we etched the Au–Zn–Au films by Ar ion beam etching and semiconductors to just above the n-GaInAs layer

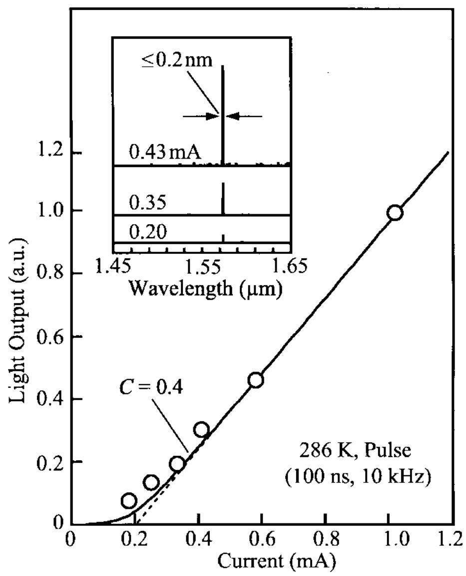

Fig. 2. Theoretical curve and experimental plots of light output versus current characteristic, and lasing spectra of 2-μm-diameter device.

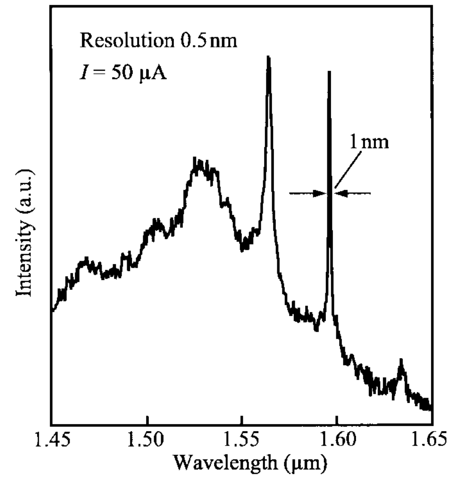

Fig. 3. Spontaneous emission spectra observed for 3-μm-diameter device under CW condition at 286 K.

by methane-based reactive ion beam etching (RIBE) [9]. Formed circular mesas were nearly 4 μm in height. From the topographic image by field emission scanning electron microscope (SEM), the roughness of side walls was measured to be 5 nm or less. After annealing the wafer for making ohmic contact, we formed the disk shape by selective wet etching of InP claddings using HCl solution at 2 °C. The disk width projecting from the center region supported by remained InP pedestals can be 1 μm for etching time approximated by $13D$ [s], where D is the disk diameter in the unit of micrometers. To manage both sufficient carrier diffusion into the disk edge and suppression of scattering loss at the edge of InP pedestals, we controlled the disk width of all the devices to 0.5–1 μm for maintaining whispering gallery modes. Fig. 1 shows a side view of the 2-μm-diameter device. The diameter of top contact was reduced to 1.2 μm by the RIBE process. The current was flowed from a tungsten probe directly touching the top contact. The light radiation was directly detected by a sharpened single-mode fiber and analyzed by an optical spectrum analyzer. For smaller devices, the radiation was uniform inside the substrate plane. For devices larger than 5 μm in diameter, it was uniform above threshold, but was slightly stronger in $\langle 110 \rangle$ and $\langle 1\bar{1}0 \rangle$ directions below threshold. This seems to be caused by the difference between the scattered radiation of whispering gallery modes above threshold and the relatively strong radiation below threshold from the center region supported by InP pedestals whose cross section has square shape for larger devices.

In Fig. 2, open circles show the light output versus current characteristic for 2-μm-diameter device observed at 286 K under pulsed condition. The threshold current was estimated to be 0.2 mA. This value seems to be at the smallest level among those reported for GaInAsP lasers, even though considering the relatively low environmental temperature. For this device, the spontaneous emission factor C [8] was calculated to be 0.4 when assuming the polarization anisotropy of CS-MQW wafer [10]. In Fig. 2, theoretical curve with $C = 0.4$ was also shown, which fits to experimental plots with small error. Excess power observed below threshold seems to be that from the center region. Above threshold, the spectrum showed single-mode lasing with FWHM of 0.2 nm, the resolution limit of the measurement. CW lasing was not obtained due to large heat caused by large series resistance of 0.6–2 kΩ and no heat sinking structure. However, some device chips exhibited sharp resonances, as shown in Fig. 3; the resonance width was 1 nm for CW current as low as 50 μA. This indicates a very high quality of the cavity.

We theoretically analyzed the lasing characteristics, taking the following features of microdisk lasers into account: 1) logarithmic gain characteristic of CS-MQW; 2) large optical confinement factor; 3) low absorption loss and long spontaneous emission lifetime [11] in semiconductor/air waveguide; 4) scattering loss and diffraction loss; 5) surface recombination at disk surfaces; 6) current passing through the center region; and 7) decay of carrier concentration toward disk edge. We noticed in the analysis that threshold current is sensitive to the surface recombination velocity v_s as well as the assumed carrier concentration N_s in GRIN layers. The minimum threshold current was 0.7 mA for $D = 3$, 0.9 mA for $D = 5$, and 2.5 mA for $D = 10$. These data almost fit to theoretical values for $v_s = 1 - 3 \times 10^4$ cm/s and $N_s = 0.2N$, where N is the carrier concentration in quantum wells. Low threshold of 40 μA is expected for $D = 1.5$ if the surface recombination is suppressed to negligible order. This may be achieved by increasing the barrier height of GRIN layers so far as the GRIN layers are not removed by the wet etching.

III. Cavity Modes and Spontaneous Emission Factor

Cavity modes of microdisk lasers were calculated by a 2-D model, in which a circular region having guided-wave equivalent index of microdisk is surrounded by an outer region having index of 1. The guided-wave equivalent index, resonant wavelength and field distribution inside the 2-D plane for mode order M were obtained by simultaneously solving the guided-wave equation and axially symmetric wave equation

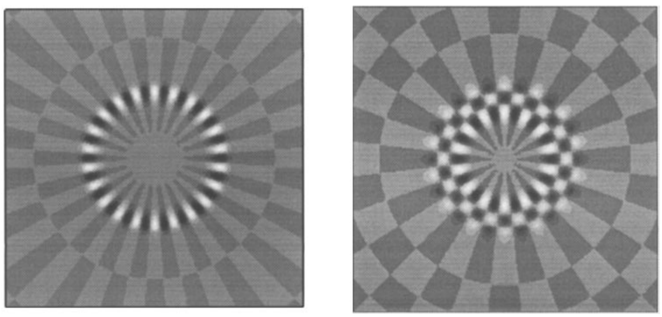

(a) (b)

Fig. 4. Simulated magnetic field distribution of cavity modes in 5-μm-diameter microdisk laser.

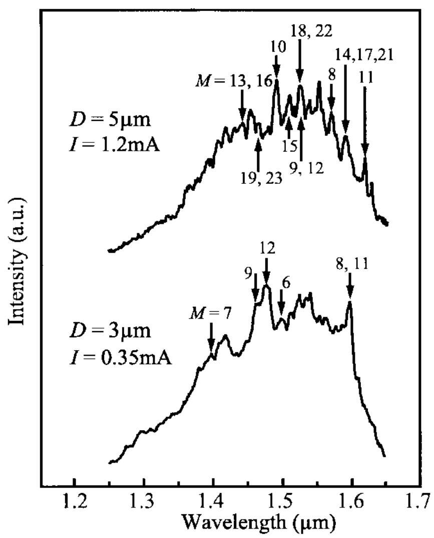

Fig. 5. Spontaneous emission spectra observed for different disk diameters under CW condition.

with boundary conditions. Fig. 4 shows some examples of magnetic field distribution in 5-μm-diameter microdisk. Here, the electric field vector is fixed inside the 2-D plane since it almost simulates the polarized emission in CS-MQW [10]. Fig. 4(a) displays typical whispering gallery modes. The difference of resonant wavelength of such modes is 63 nm and this value increases by reducing the disk diameter. Fig. 4(b) displays lower order modes, which have resonant wavelengths close to that of Fig. 4(a) and maximum amplitude relatively inside the disk. If the disk width of actual devices is wider than 1 μm, lower order modes acquire low loss condition and high gain, resulting in multimode lasing operation. Although we showed single-mode lasing spectra in Fig. 2, we also observed multimode lasing in many device chips with diameter of larger than 5 μm.

Fig. 5 shows spontaneous emission spectra under CW condition and arrows indicate resonant wavelengths calculated for mode order M. It is seen that many peaks observed well coincide with calculated resonant wavelengths, and that the number of peaks simply decreases as the disk diameter decreases. The spectral width $\Delta\lambda$ of these spectra was as wide as 200 nm. This seems to be caused by the heat under cw condition. If the spectral width is reduced to less than 100 nm, which is typical for quaternary lasers, the number of modes in the spectra will be limited to 4–5. Disk diameter less than 1.5 μm will satisfy the single-mode condition of spontaneous emission except for a small amount of free mode radiation in the vertical direction. On this condition, the spontaneous emission factor reaches 0.5 [8], the upper limit for single polarization, or larger for the polarized spontaneous emission from CS-MQW. The effective cavity volume calculated from the distribution of whispering gallery mode in the 2-μm-diameter device was estimated to be 0.4 μm^3. This value seems to be the smallest among those for any types of electrically pumped lasers ever reported.

IV. Conclusion

We have demonstrated the smallest microdisk injection laser with low threshold current of 0.2 mA. Further reduction of disk diameter to less than 1.5 μm will achieve large spontaneous emission factor close to 1. The size will soon be realized by improvements on the RIBE process. CW lasing and suppression of surface recombination at disk surfaces are key issues to clearly evaluate the spontaneous emission factor and expected effects of spontaneous emission control.

Acknowledgment

The authors would like to than Prof. Y. Kokubun, Yokohama National University, Japan, and Prof. K. Iga and Prof. F. Koyama, Tokyo Institute of Technology, Japan, for encouragement and discussion. They also thank Dr. A. Kasukawa, Furukawa Electric Co., Ltd., Japan.

References

[1] T. Kobayashi, Y. Morimoto, and T. Sueta, "Closed microcavity laser," in *Nat. Top. Meet. Rad. Sci.*, 1985, no. RS85-06 (in Japanese).

[2] E. Yablonovitch, "Inhibited spontaneous emission in solid-state physics and electronics," *Phys. Rev. Lett.*, vol. 58, pp. 2059–2062, 1987.

[3] Y. Yamamoto, S. Machida, K. Igeta, and G. Björk, "Controlled spontaneous emission in microcavity semiconductor lasers," *Coherence, Amplification, and Quantum Effects in Semiconductor Lasers*, Y. Yamamoto, Ed. New York, Wiley Interscience, 1991, pp. 561–615.

[4] H. Yokoyama and K. Ujihara, Eds., *Spontaneous Emission and Laser Oscillation in Microcavities*. New York, CRC, 1995.

[5] A. F. J. Levi, R. E. Slusher, S. L. McCall, T. Tanbun-Ek, D. L. Coblentz, and S. J. Pearton, "Room temperature operation of microdisk lasers with submilliamp threshold current," *Electron. Lett.*, vol. 28, pp. 1010–1012, 1992.

[6] S. L. McCall, A. F. J. Levi, R. E. Slusher, S. J. Pearton, and R. A. Logan, "Whispering gallery mode microdisk lasers," *Appl. Phys. Lett.*, vol. 60, pp. 289–291, 1992.

[7] A. F. J. Levi, S. L. McCall, S. J. Pearton, and R. A. Logan, "Room temperature operation of submicrometer radius disk laser," *Electron. Lett.*, vol. 29, pp. 1666–1667, 1993.

[8] T. Baba, T. Hamano, F. Koyama, and K. Iga, "Spontaneous emission factor of a microcavity DBR surface emitting lasers," *IEEE J. Quantum Electron.*, vol. 27, pp. 1347–1358, 1991.

[9] T. Baba, N. Kamizawa, and M. Ikeda, "Nanofabrication process of GaInAsP/InP 2D photonic crystals by a methane-based reactive ion beam etching technique," *Physica B*, vol. 227, pp. 415–418, 1996.

[10] E. P. O'Reilly and A. R. Adams, "Band-structure engineering in strained semiconductor lasers," *IEEE J. Quantum Electron.*, vol. 30, pp. 366–379, 1994.

[11] E. Yablonovitch, T. J. Gmitter, and R. Bhat, "Inhibited and enhanced spontaneous emission from optically thin AlGaAs/GaAs double heterostructure," *Phys. Rev. Lett.*, vol. 61, pp. 2546–2549, 1988.